

## **FRACTURE TOUGHNESS AND MICROSTRUCTURE OF CONCRETE AT EARLY-AGES**

**Zongjin Li (1), Xianyu Jin (2) and Chen Lin (2)**

(1) Dept. of Civil Engineering, Zhejiang University, Hangzhou, China

(2) Dept. of Civil and Environmental Engineering, Hong Kong University of Sci. and Tech.,  
Hong Kong, China

### **Abstract**

This paper reports the results of a study on fracture behavior of concrete at early ages. The two-parameter fracture model has been used to determine the fracture toughness  $K_{Ic}^s$  and critical crack tip opening displacement ( $CTOD_c$ ). Meanwhile, microstructure parameters such as pore size distribution have been studied by mercury intrusion porosimetry (MIP). The parameters were obtained for three types of concretes at different ages from 18 hours to 28 days. It was found that  $K_{Ic}^s$  increases with hydration time, but porosity changes in the opposite way. The lower water-cement ratio led to a more rapid development of  $K_{Ic}^s$  at early ages. There existed a close relationship between  $K_{Ic}^s$  and porosity. In addition, the interfaces between coarse aggregate and cement matrix were studied by scanning electron microscopy (SEM) at the age of 28 days to interpret its influence to mechanical properties.

**Keywords:** compressive strength; fracture toughness; concrete, porosity; ITZ.

### **1. INTRODUCTION**

Since linear elastic fracture mechanics (LEFM) was first applied to concrete by Kaplan in 1961 [1], many investigations have been conducted to measure the apparent values of fracture toughness  $K_{Ic}$  for cement paste, mortar, and concrete specimens. A great deal of test results showed that  $K_{Ic}$  was dependent of specimen geometry and size. It implied that the fracture toughness  $K_{Ic}$  based on LEFM and brittle fracture concepts could not be directly applied to materials such as concrete [2].

With the development of nonlinear fracture mechanics (NLFM) of concrete, which took fracture process zone (FPZ) of concrete into consideration, RILEM had tentatively recommended three equivalent effective crack models Jenq and Shah's two-parameter model (TPM), Bazant's size effect law (SEL), and effective crack model (ECM) by Karihaloo and Nallathambi [3,4], for determining the fracture parameters of concrete, which were material constants, and independent of geometry and size.

Most of the related literatures focused on the fracture properties of mature concrete. However, it was known that the properties at early age (generally referring to age less than 7 days) had great influence the long-term behavior and was critical for construction quality control. Recently, Zolinger et al. [5] measured two fracture parameters, the fracture toughness  $K_{Ic}^b$  and the critical effective crack length of the FPZ  $c_f$ , for concrete at 0.5, 1, 7, 21, and 28 days, and concluded that  $K_{Ic}^b$  increased with hydration process.

In current study, experimental investigations have been conducted on concrete at early age using beam specimens with three different mix proportions. The fracture parameters have been obtained with two parameter model at 18 hours, 1, 2, 7 and 28 days.

From a materials science point of view, properties at one level could be explained by the characterizations of lower level. Unlike compressive strength, there were not too many literatures dealing with the relationship between microstructure and fracture characteristics of concrete.

Although with some limitations, in all the methods applied to explore the pore structure, MIP becomes the most extensively used, for its simplicity and large range of pore diameter accessed (about 30-360 $\mu$ m) [6].

In this paper, pore structure was studied by MIP using the samples sawed from the ruptured beams. The results showed that  $K_{Ic}^s$  increased with hydration time while the porosity value decreased with hydration process. There existed a negative relationship between these two quantities.

## 2. EXPERIMENTAL PROGRAM

### 2.1 Materials

Cement: ASTM Type I Portland cement, with specific gravity of 3.15 and specific surface area of 385 m<sup>2</sup>/kg. The average particle size of cement is 19.98  $\mu$  m.

Fine aggregate: Natural river sand with a fineness modulus of 2.3, and specific gravity of 2.66. Coarse aggregate: Crushed aggregate with maximum size of 10mm and specific gravity of 2.57. Silica fume: Compatible silica fume with average particle size 0.1  $\mu$  m. Water: Tap water. Superplasticizer: KFDN (produced by Zhaoshen Building Chemical (Shenzhen) Co. Ltd).

### 2.2 Mix proportion

Three different mix proportions of concrete are summarized in Table 1.

**Table1: Concrete mix proportions**

	Binder		Fine aggregate	Coarse aggregate	Water	Superplasticizer*	W/B
	Cement	Silica fume					
NSC	1	-	2.0	2.7	0.55	-	0.55
MSC	1	-	1.7	2.5	0.40	0.4%	0.44
HSC	0.9	0.1	1.0	1.8	0.30	0.8%	0.30

\* Percentage of by weight of binder

### 2.3 Specimens preparation

At least four beams with a precast notch were prepared for each batch of concrete. The specimen dimensions were summarized as follows: 75mm in width (B), 150mm in depth (D), and 750 mm in length (L). The depth of notch (initial crack length,  $a_0$ ) was 50mm, and the width 3mm. More details could be found in Fig. 1.

Details of batching, casting, consolidating, and curing were summarized herein. A pan mixer was used for mixing. The beam specimens were cast in reusable moulds and consolidated with vibrator.

After fully consolidation, all specimens were troweled and cured under polyethylene membrane in a laboratory environment for 24 hours except the specimens tested at 18 hours and 1 day. Specimens were then removed from the moulds and transferred to a curing room with the temperature of  $23 \pm 2^\circ\text{C}$  and relative humidity of 100% until about 4 hours before test. All the operations conformed to ASTM C192/C 192M – 98.

Two cubes with  $13 \pm 1\text{mm}$  per side were cut from the ruptured beam specimen with a water-cooled, diamond-bladed saw as soon as the fracture test was over. Then the samples were dried in an oven at a temperature of  $105\text{-}110^\circ\text{C}$  for 24 hours or more to a constant weight. After drying, the samples were kept in desiccators till test.

### 2.4 Instrumentation

All beams were loaded using MTS 810 in three-point bending, a 250-kN hydraulic closed-loop mechanics test systems. Crack mouth opening displacement (CMOD) was used as feedback signal to achieve a stable failure. A high-speed data acquisition system was used to collect the necessary data.

For MIP, Micromeritics Autopore IV 9500 with capacity of 207 MPa (30,000 psia) was used. The range of diameter accessed was from  $0.006\mu\text{m}$  to  $360\mu\text{m}$ .

JEOL-6300 SEM (Model JSM 6300) was used in SEM study.

## 3. TWO-PARAMETER MODEL

According to the proposal of RILEM, The modulus of elasticity could be obtained as follows:

$$E = 6Sa_0V_1(\alpha)/(C_iD^2B) \quad (1)$$

Where S, B, D and  $a_0$  were span, thickness, height and initial notch depth respectively and  $C_i$  was the initial compliance as illustrated in Fig. 1.  $V_1$  was a geometrical function of  $\alpha$ :

$$V_1(\alpha) = 0.76 - 2.28\alpha + 3.87\alpha^2 - 2.04\alpha^3 + 0.66/(1-\alpha)^2 \quad (2)$$

in which,  $\alpha = (a_0 + H_0)/(D + H_0)$ ,  $H_0$  was the height of clip gauge holder.

The fracture toughness  $K_{Ic}^s$  was given by:

$$K_{Ic}^s = \frac{3(P_{\max} + 0.5WS/L)S}{2D^2B} \sqrt{\pi a_e} F(\alpha) \quad (3)$$

where W and L were the self-weight and length of beam respectively.  $P_{\max}$  was the maximum load. And  $a_e$  was the critical crack length, which is determined by iteration from:

$$a_e = EC_u D^2 B / 6SV_1(\alpha) \quad (4)$$

in which,  $\alpha = (a_e + H_0) / (D + H_0)$ , the geometrical function F was given by:

$$F(\alpha) = [1.99 - \alpha(1 - \alpha)(2.15 - 3.93\alpha + 2.7\alpha^2)] / [\sqrt{\pi}(1 + 2\alpha)(1 - \alpha)^{3/2}] \quad (5)$$

And  $C_u$  was the unloading compliance.

Finally, the critical crack tip opening displacement  $CTOD_c$  was given by:

$$CTOD_c = \frac{6(P_{max} + 0.5WS/L)Sa_e}{D^2 BE} V_1(\alpha) \{ (1 - \beta)^2 + (-1.149\alpha + 1.081)(\beta - \beta^2) \}^{1/2} \quad (6)$$

in which,  $\alpha = a_e / D$ ,  $\beta = a_0 / a_e$ .

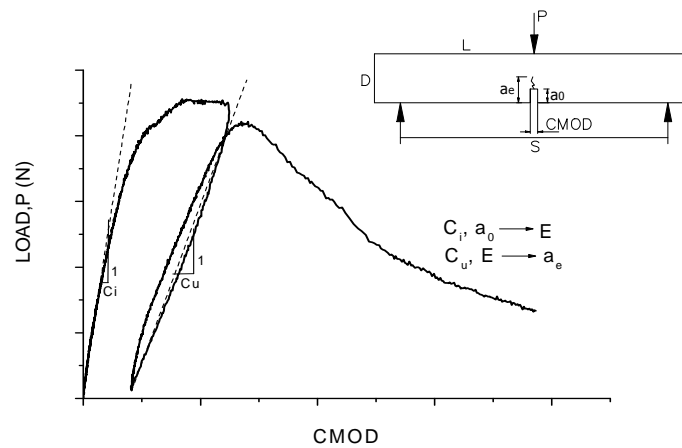


Figure 1: Typical load-CMOD plot

#### 4. EXPERIMENTAL RESULTS AND DISCUSSIONS

Test results and analyses were shown in Table 2 and Table 3. The meaning of the notations was summarized as follows:  $f'_c$  - uniaxial compressive strength;  $E_c$  - modulus of elasticity in compression;  $f_t$  - splitting tensile strength;  $K_{Ic}^s$  - fracture toughness;  $CTOD_c$  - critical crack tip opening displacement;  $G_{Ic}^s$  - critical strain energy release rate,  $G_{Ic}^s = K_{Ic}^s{}^2 / E$ ;  $l_{ch}$  - characteristic length defined in Hillerborg's Fictitious Crack Model [12],  $l_{ch} = (E \bullet G_F / f_t^2)$ , according to Planas and Elices [13],  $G_F = \alpha G_{Ic}^s$ ,  $\alpha$  was a constant and  $\alpha > 2$ .

**Table 2: Compressive strength, Splitting tensile strength and modulus of elasticity at different ages**

(a) NSC

Age (Day)	$f'_c$ (MPa)	$E_c$ (GPa)	$f'_t$ (MPa)	$f'_c / f'_t$
0.75	8.42	10.11	1.73	4.87
1	10.46	11.61	2.85	3.67
2	15.30	15.81	3.26	4.69
7	25.66	18.00	3.70	6.93
28	35.97	23.55	3.83	9.40

(b) MSC

Age (Day)	$f'_c$ (MPa)	$E_c$ (GPa)	$f'_t$ (MPa)	$f'_c / f'_t$
0.75	16.00	16.19	2.05	7.79
1	18.61	17.26	2.47	7.52
2	26.15	21.48	2.80	9.35
7	37.53	23.99	3.61	10.40
28	57.37	29.01	4.24	13.53

(c) HSC

Age (Day)	$f'_c$ (MPa)	$E_c$ (GPa)	$f'_t$ (MPa)	$f'_c / f'_t$
0.75	27.80	19.49	3.31	8.39
1	32.23	19.86	3.38	9.53
2	44.85	23.04	4.38	10.23
7	62.68	26.85	4.83	12.99
28	84.15	31.71	5.60	15.02

**Table 3: Fracture parameters and material brittleness of MSC concretes at different ages**

Age (Day)	$K_{Ic}^s$ (MPa $\sqrt{m}$ )	$CTOD_c$ (mm)	$G_{Ic}^s$ (N/m)	Q (mm)
0.75	0.5588	0.0115	18.22	111.0
1	0.6901	0.0131	24.91	107.4
2	0.7771	0.0128	27.34	125.2
7	1.0371	0.0126	35.06	84.9
28	1.3328	0.0139	47.73	91.5

**Table 4: Fracture parameters and material brittleness at 28 days for different concretes**

Age (Day)	$K_{Ic}^s$ (MPa $\sqrt{m}$ )	$CTOD_c$ (mm)	$G_{Ic}^s$ (N/m)	Q (mm)
NSC	1.2630	0.0159	50.24	108.91
MSC	1.3328	0.0139	47.73	91.5
HSC	1.1147	0.0144	46.97	88.6

#### 4.1 Compressive Strength and Tensile Strength

As we expected, the compressive strength, splitting tensile strength and modulus of elasticity increased with the hydration process (see Fig. 3). But the developing rates for the three quantities were different. Increase of the ratio of  $f_t$  to  $f_c$  with age was found in three concretes, which indicated the lower developing rate of tensile strength. This was true for  $E_c$ . The lower the w/c ratio, the higher the values of compressive strength, splitting tensile strength and modulus of elasticity at the same time. However, the ratio of  $f_t$  to  $f_c$  decreased with the decrease of w/c ratio. These values were about 1/10, 1/14 and 1/15 for NSC, MSC and HSC respectively for example.

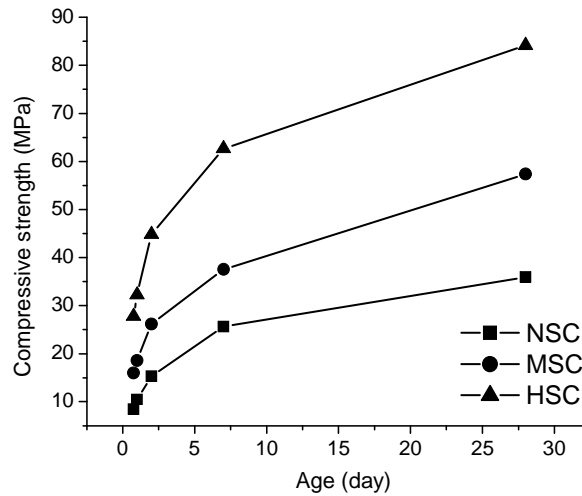


Figure 2: Development of compressive strength with hydration age

#### 4.2 Fracture Toughness and Material Brittleness

As shown in Fig. 4, fracture toughness increased with the hydration process. On the contrary, the  $CTOD_c$  value just had little development with the increase of hydration age, especially in MSC and HSC. At the same time, the developing rates of  $K_{Ic}^s$  value were distinct with varied w/c ratio and admixture dosage. The lower w/c ratio, the more rapidly  $K_{Ic}^s$  increase at early age. For instance, the ratio of  $K_{Ic}^s$  at 7 days to that at 28 days are 77.3%, 77.8% and 84.8% for NSC, MSC and HSC respectively. Also, the  $K_{Ic}^s$  value increased in the sequence of NSC, MSC and HSC at the same age.  $K_{Ic}^s$  and  $CTOD_c$  values from different specimens were in good agreement, which implies that  $K_{Ic}^s$  and  $CTOD_c$  determined by TPM could be regarded as material constants independent of geometry and size. Based on Fig. 3, it seemed that the relationship between fracture toughness  $K_{Ic}^s$  and compressive strength  $f_c$  was bi-linear, independent of w/c ratio and hydration age.

Although  $K_{Ic}^s$  increased with decreased w/c ratio, fracture behavior of the specimens with lower w/c ratio was more brittle. Therefore  $K_{Ic}^s$  was not an appropriate parameter for characterizing the fracture behavior of quasi brittle materials such as concrete. Shah had proposed the materials length, Q, to determine the brittleness of concrete in his fictitious crack

model. The lower the Q value, the more brittle the material. Generally speaking, the Q decreased with the hydration age, which showed early-age concrete is more ductile than mature one as shown in Table 3. The Q values at 28 days for three concretes were summarized in Table 4. We have known that high strength concrete behaves more brittle than normal strength concrete. This can be roughly justified from the test results.

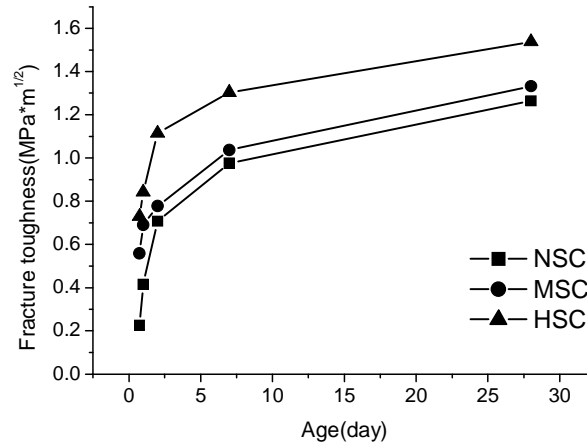


Figure 3: Development of fracture toughness with hydration age

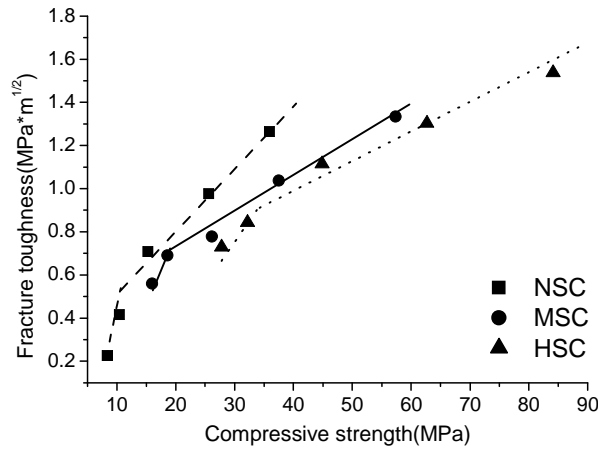


Figure 4: Relationship between fracture toughness and compressive strength

### 4.3 Pore Structure

It's generally accepted that bulk mechanical properties are directly related to the void content of materials, not only concrete [7]. We try to obtain some links between the porosity and strength of concrete in this section. The MIP results are summarized in Table 5 and Fig. 5. The total porosity decreases with hydration ages and w/c ratio. At the same time, the proportion of finer pores increases, which means the improvements of mechanical properties, according to Mindess [8]. The test results verify this point. Fig. 5 and Fig. 6 show the relationships between the porosity P and compressive strength  $f'_c$  and  $K_{Ic}^s$ . The lower the porosity, the higher  $f'_c$  value. This is true for P and  $K_{Ic}^s$ . There exists a linear relationship with negative slope

coefficient between  $K_{Ic}^s$  and porosity, viz.  $K_{Ic}^s = aP + b$ ,  $a$  is a negative number. Although further studies need to carry out, it's clear that, like compressive strength, the fracture toughness depends directly on porosity too.

**Table 5: Porosity (per cent) of three concretes at different ages**

Age	18h	2d	7d	28d
NSC	18.88	13.45	10.40	8.16
MSC	14.40	11.19	9.14	7.15
HSC	13.35	9.55	6.75	6.07

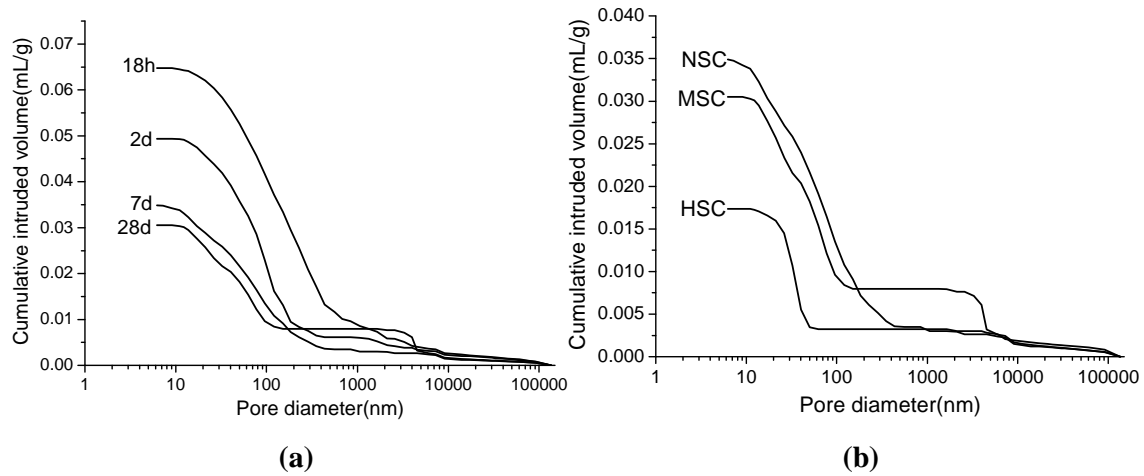


**Figure 5: Pore size distribution curves of (a) MSC at different ages, (b) of three concretes at 28 days.**

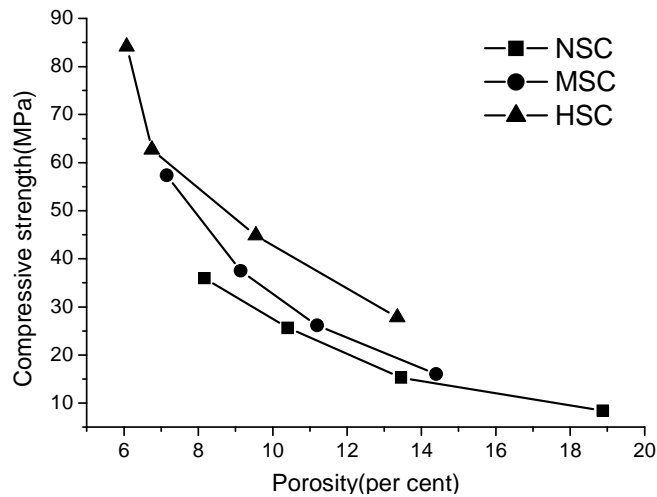


**Figure 6: Relationship between compressive strength and porosity**

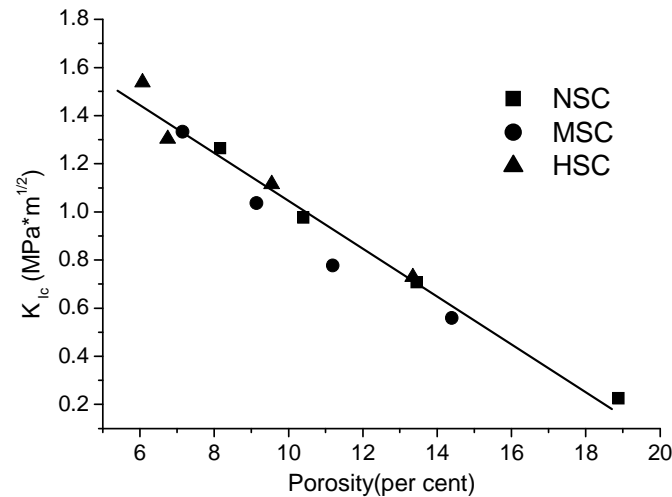


**Figure 7: Relationship between fracture toughness and porosity**

#### 4.4 Aggregate-Matrix Interfaces

On account of some reasons, such as wall-effect and flow of water, the interfacial transition zone (ITZ) between aggregate and cement paste has a water film formed during mixing process. This results in an increase of porosity, which makes ITZ to be a weak part of concrete. Additionally, micro-cracks exit because of the mismatch between aggregate and cement matrix. Fig. 8 shows the images of the interfaces in three concretes at 28 days. The micro-cracks can be observed obviously. We found that the failure occurred around coarse aggregate in NSC and MSC, which means that ITZ is the weakest link in these two concretes. The micro-cracks become smaller and the bond in ITZ is enhanced with decrease of w/c ratio. This makes MSC have better mechanical properties (compressive strength, fracture toughness, etc.) than NSC. But for HSC, the case is not true. The reasons may be twofold. On one hand, the w/c ratio decreases. On the other hand, this maybe attributes to use of silica fume. First of all, there is the fine particle effect. Silica fume will reduce the pore-space, which has a positive effect on strength. Second, the silica fume will react with the calcium hydroxide in ITZ, so-called pozzolanic effect, which also reduces the porosity of the interface. [9-11] In a word, the decrease of w/c ratio and the positive effect of silica fume lead to the increase of bond strength of ITZ, which make difference in mechanical parameters of the three concretes

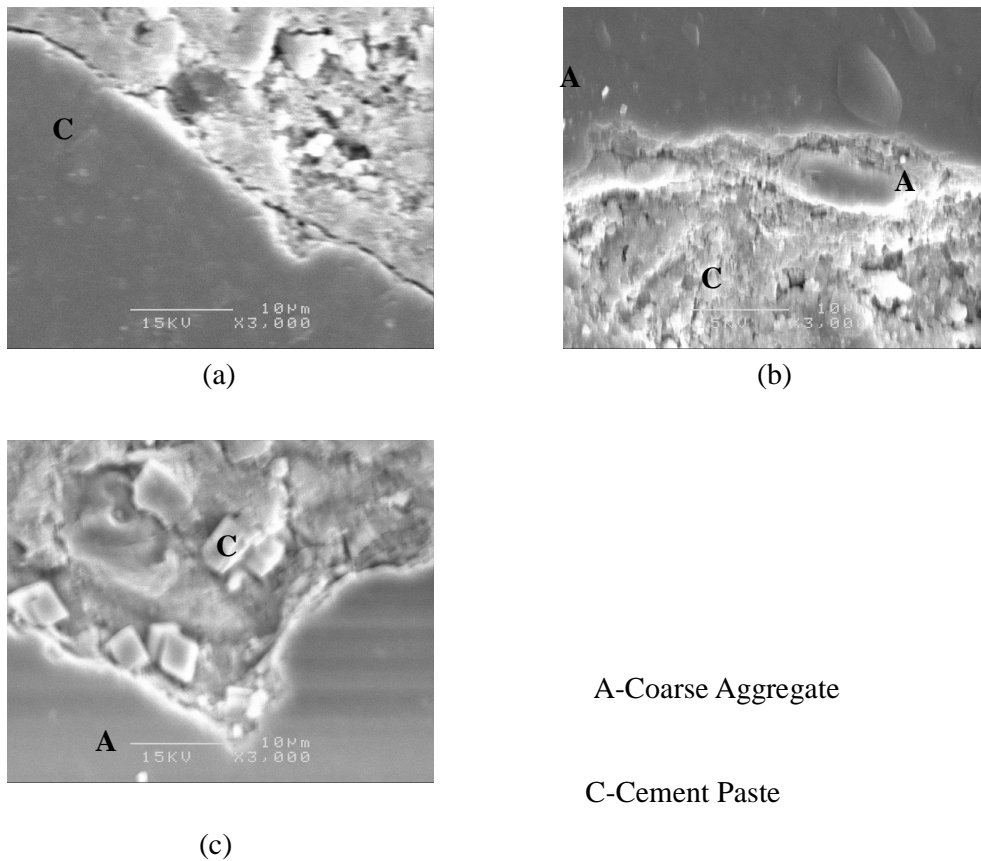


**Figure 8: SEM Images at 28 days (a) NSC, (b) MSC, (c) HSC**

## 5. CONCLUSIONS

In light of the experimental measurements of fracture properties, the investigations of pore structure and the aggregate-matrix interfaces; the following conclusions can be drawn.

- The values of  $f_c^s$ ,  $E_c$ ,  $f_t$  and  $K_{lc}^s$  increase with the hydration age from 18 hours to 28 days. The lower w/c ratio, the more rapidly the four quantities increase at early age. Increasing  $K_{lc}^s$  indicates the resistance to cracking increase with the age for three concretes.
- Increase of the characteristic length with the hydration age implies that early-age concrete is more brittle than mature concrete. The lower w/c, the more brittle the concrete at 28 days, according to the Q values.
- The relationship between fracture toughness  $K_{lc}^s$  and compressive strength  $f_c^s$  seems to be bilinear, regardless of w/c ratio.
- The higher the porosity, the lower compressive strength and fracture toughness. The relationship between these two quantities is linear, viz.  $K_{lc}^s = aP + b$ ,  $a$  is a negative number.

- The aggregate-matrix interfacial zone becomes denser with lower w/c ratio and the use of silica fume. It's an essential ways to get concrete with high fracture properties to add mineral admixture such as silica fume.

## ACKNOWLEDGMENTS

The authors gratefully acknowledge the financial support of key project from National Natural Science Foundation of China (50838008) and the Grant from Research Grant Council (616008).

## REFERENCES

- [1] Kaplan, M.F., "Crack Propagations and the Fracture of Concrete," *ACI Journal*, Proceedings V.58, No. 11, Nov. 1961, pp. 591-610.
- [2] Bazant, Z. P. and J. Planas, *Fracture and Size Effect in Concrete and Other Quasibrittle Materials*, *CRC Press*, New York, 1998.
- [3] Shah, S. P. and Carpinteri, A., *Fracture Mechanics Test Methods for Concrete*, *RILEM Report 5*, Chapman and Hall, London, 1991, pp. 1-69.
- [4] Jenq, Y. S. and S. P. Shah, "Two Parameter Fracture Model for Concrete," *Journal of Engineering Mechanics*, V.111, No. 10, Oct. 1985, pp.1227-1241.
- [5] Zolinger D a n G., Tang Tianxi, and Yoo Rae H., "Fracture Toughness of Concrete at Early Ages," *ACI Materials Journal*, V. 90, No. 5, Sep.-Oct. 1993, pp. 463-471.
- [6] Kumar Rakesh, Bhattacharjee B., "Study on some factors affecting the results in the use of MIP method in concrete research," *Cement and Concrete Research*, V. 33, Issue 3, 2003, pp. 417-424.
- [7] Neville A. M., *Properties of Concrete*, *Fourth and Final Edition*, J. Wiley & Sons, New York, pp. 277-284.
- [8] Mindess, S. "Relationships between strength and microstructure for cement-based materials: an overview," *Very High Strength Cement-Based Materials* (J. F. Young Editor), *Symposia Proceeding*, Materials Research Society, Vol. 42, 1984, pp. 53-68.
- [9] Jan G. M. van Mier, *Fracture Processes of Concrete*, *CRC Press*, New York, 1997, pp. 33-52.
- [10] Maso J. C. (Editor), *Interfacial Transition Zone in Concrete*, *RILEM Report 11*, E & FN SPON, London, 1996.
- [11] Ji Yajun, Jong Herman Cahyadi, "Effects of densified silica fume on microstructure and compressive strength of blended cement pastes," *Cement and Concrete Research*, V. 33, Issue 10, 2003, pp. 1543-1548.